LETTERS

Shell-isolated nanoparticle-enhanced Raman spectroscopy

Jian Feng Li[1], Yi Fan Huang[1], Yong Ding[2], Zhi Lin Yang[1], Song Bo Li[1], Xiao Shun Zhou[1], Feng Ru Fan[1,2], Wei Zhang[1], Zhi You Zhou[1], De Yin Wu[1], Bin Ren[1], Zhong Lin Wang[2] & Zhong Qun Tian[1]

Surface-enhanced Raman scattering (SERS) is a powerful spectroscopy technique that can provide non-destructive and ultrasensitive characterization down to single molecular level, comparable to single-molecule fluorescence spectroscopy[1–15]. However, generally substrates based on metals such as Ag, Au and Cu, either with roughened surfaces or in the form of nanoparticles, are required to realise a substantial SERS effect, and this has severely limited the breadth of practical applications of SERS. A number of approaches have extended the technique to non-traditional substrates[14,16,17], most notably tip-enhanced Raman spectroscopy (TERS)[18–20] where the probed substance (molecule or material surface) can be on a generic substrate and where a nanoscale gold tip above the substrate acts as the Raman signal amplifier. The drawback is that the total Raman scattering signal from the tip area is rather weak, thus limiting TERS studies to molecules with large Raman cross-sections. Here, we report an approach, which we name shell-isolated nanoparticle-enhanced Raman spectroscopy, in which the Raman signal amplification is provided by gold nanoparticles with an ultrathin silica or alumina shell. A monolayer of such nanoparticles is spread as 'smart dust' over the surface that is to be probed. The ultrathin coating keeps the nanoparticles from agglomerating, separates them from direct contact with the probed material and allows the nanoparticles to conform to different contours of substrates. High-quality Raman spectra were obtained on various molecules adsorbed at Pt and Au single-crystal surfaces and from Si surfaces with hydrogen monolayers. These measurements and our studies on yeast cells and citrus fruits with pesticide residues illustrate that our method significantly expands the flexibility of SERS for useful applications in the materials and life sciences, as well as for the inspection of food safety, drugs, explosives and environment pollutants.

The invention of TERS led to a breakthrough in the substrate and surface generalities of SERS[18,19]. It uses a working mode that separates the probed substance from a Au tip that acts as the Raman signal amplifier (Fig. 1a–c). The largely enhanced electromagnetic field generated on the probe tip under the excitation of a suitable laser can extend to the sample that is in close proximity to the tip apex. In principle, the Raman signals from any substrate regardless material and surface smoothness can be enhanced by the tip apex with high spatial resolution[19]. However, the total Raman scattering signal from the tip area (about 20–50 nm in diameter) is rather weak, so TERS studies have been largely limited to molecules having large Raman cross-sections. Moreover, its instrument is sophisticated and expensive, making it impractical for many applications.

Our approach is to replace the Au tip by a monolayer of Au nanoparticles (Fig. 1d), each coated with an ultrathin shell of silica or alumina (here denoted Au/SiO₂ or Au/Al₂O₃ nanoparticles). Each

nanoparticle acts as an Au tip in the TERS system, and thus this technique simultaneously brings thousands of TERS tips to the substrate surface to be probed (Supplementary Fig. 3). We can obtain the jointly enhanced Raman signal contributed by all of these nanoparticles, which is two to three orders of magnitude higher than that for a single TERS tip. Moreover, the use of a chemically inert shell coating around the Au nanoparticle protects the SERS-active nanostructure from contact with whatever is being probed. The main virtue of such a shell-isolated mode is its much higher detection sensitivity and vast practical applications to various materials with diverse morphologies. We call this new technique shell-isolated nanoparticle-enhanced Raman spectroscopy (SHINERS).
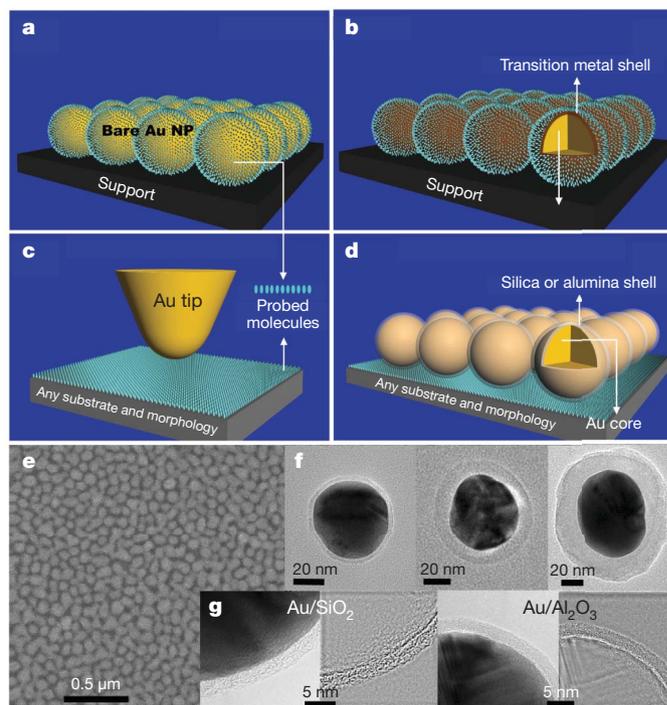

Figure 1 | The working principles of SHINERS compared to other modes. Schematic of the contact mode. **a**, Bare Au nanoparticles: contact mode. **b**, Au core–transition metal shell nanoparticles adsorbed by probed molecules: contact mode. **c**, Tip-enhanced Raman spectroscopy: non-contact mode. **d**, SHINERS: shell-isolated mode. **e**, Scanning electron microscope image of a monolayer of Au/SiO₂ nanoparticles on a smooth Au surface. **f**, HRTEM images of Au/SiO₂ core–shell nanoparticles with different shell thicknesses. **g**, HRTEM images of Au/SiO₂ nanoparticle and Au/Al₂O₃ nanoparticle with a continuous and completely packed shell about 2 nm thick.

[1]State Key Laboratory of Physical Chemistry of Solid Surfaces and College of Chemistry and Chemical Engineering, Xiamen University, Xiamen 361005, China. [2]School of Materials Science and Engineering, Georgia Institute of Technology, Atlanta, Georgia 30332–0245, USA.

We rationally designed gold nanoparticles coated with a thin, uniform, fully enclosed and optically transparent shell of silica or alumina so that the gold core generates a large surface enhancement, and so that the shell controls the distance of the core from the surface to be studied. The physical property (strong electromagnetic field) of the Au nanoparticles is thus transferred to enhance the chemical signal, for example, Raman vibrational bands, of the molecules on the material surfaces we are examining. Moreover, the chemically inert shell ensures that there is no direct contact between the probed substance and the gold core. To prepare the shell-isolated nanoparticles, Au nanoparticles with a diameter of ~55 nm were synthesized as cores[21], onto which ultrathin silica shells were coated to form Au/SiO$_2$ nanoparticles[22–25], which were then spread onto sampled surfaces as a monolayer for measurement (Fig. 1e).

To elaborate the principle of SHINERS, we carried out a systematic study on the Raman scattering intensity as a function of the silica shell thickness from 2 to 20 nm. The experimental data are in good agreement with the three-dimensional finite-difference time-domain calculated result[26] (Supplementary Figs 4 and 5). The calculated results reveal that the magnitude of the maximally enhanced electric field is about 85 times greater for the 4-nm shell and about 142 times greater for the 2-nm shell than that of the incident light; the highest enhancement of Raman scattering appears at the junction between the particle and the substrate as hot spots with magnitudes of about 5×10^7 and 4×10^8 fold, respectively. We now present the applications of SHINERS to a few unusual cases in which the TERS technique shows either undetectable or extremely low signals.

We first applied SHINERS on the atomically flat single-crystal surfaces of different materials in the aqueous solution or electrochemical environment, which hardly produces a detectable Raman signal using existing techniques. Hydrogen adsorption is a very important system in surface science, chemistry and industry, including fuel cell applications. To our knowledge, no Raman spectrum of any hydrogen adsorbed at single-crystal surfaces has been reported because of its extremely low Raman cross-section. We spread the Au/SiO$_2$ nanoparticles over a Pt(111) single-crystal electrode in 0.1 M NaClO$_4$ and applied the electrode potential in the region of the hydrogen evolution reaction. As can be seen in Fig. 2a from curves I, II and III, a broad band at about 2,023 cm^{-1} was observed, being attributed to the Pt–H stretching vibration mode according to the previous reports on highly roughened Pt surfaces[17]. In addition, we collected Raman signals on Pt(111) under the same conditions but without Au/SiO$_2$ nanoparticles. No Raman peak in this frequency region can be observed (curve IV). Then, when we changed the shell thickness from 2 to 20 nm, the surface Raman signal also disappeared (curve V), illustrating that the ultrathin shell for the Au/SiO$_2$ nanoparticles is essential to extend the strong electromagnetic field from the Au core to the probed surface. Taken together, our data suggest that the Au/SiO$_2$ nanoparticles with the ultrathin configuration are necessary to obtain the Pt–H signal with two additional lines of evidence.

To examine the capability of SHINERS to distinguish two different single-crystal facets, we have analysed the potential-dependent Raman spectra for different single-crystal surfaces of the same metal (Au). As far as we know, it is the first time high-quality surface Raman signals have been obtained for ions such as SCN$^-$ adsorbed at Au(111) and Au (100) in an electrochemical environment. One advantage of SHINERS over surface infrared spectroscopy is that it provides direct vibrational information about the metal–molecule bonds (in the low-frequency region of Supplementary Fig. 6).

To illustrate that the shell can easily be changed from silica to other materials, we coated the Au nanoparticles with an ultrathin, uniform Al$_2$O$_3$ layer, using the atomic layer deposition method[5] (see Supplementary Methods for details), and performed the same experiment. The SHINERS spectra obtained from 55-nm Au/2-nm Al$_2$O$_3$ nanoparticles spread over Pt(111) (see Fig. 2b) have spectral features almost identical to those from the silica-coated nanoparticles, indicating that changing the shell material is feasible and the quality of the data are preserved.

To examine the capability of SHINERS for non-metallic materials, we used an atomically flat silicon (Si) wafer, used widely in the semiconductor industry (Fig. 2c). Following the basic procedure of surface treatment, the Si sample was first treated with H$_2$SO$_4$ (98%), then decorated with Au/SiO$_2$ nanoparticles for the SHINERS measurement; no Si–H band could be detected (curve IX). The strong SHINERS signal of hydrogen binding on the Si surface can be identified after being treated with HF solution (curve X). The broad band at about 2,149 cm^{-1} is attributed to the Si–H stretching vibration mode[27]. When the sample was further cleaned using O$_2$ plasma, the Si–H band vanished (curve XI). This confirms that the Si–H bond is formed only after treatment of HF solution. There have been no SERS or TERS studies on the Si–H system on smooth Si surfaces, although there have been a few Raman studies of hydrogen bonded to highly porous Si[27]. This result shows that SHINERS has a potential application in semiconductor industrial processes.

Unlike SERS using bare Au nanoparticles or TERS using a bare Au tip, by using Au/SiO$_2$ nanoparticles we can obtain more meaningful surface Raman signals because the chemically inert shell prevents direct interaction between the probed adsorbates (or surface components) and bare Au nanoparticles or the tip, which often distorts the true vibrational information (Supplementary Figs 7, 8, 9 and 10).

SHINERS has extraordinary potential for characterizing biological structures such as living cells. Yeast cells were selected because they are one of the most extensively studied model eukaryotic organisms from genetics to biochemistry. In yeast the cell walls are of considerable interest, owing to their sensitivity towards the different biological functions of the cell. Figure 3 shows the SHINERS spectra (curves I–III) from different locations of the same sample. They are very different from the normal Raman spectra (curve V) of yeast cells, but similar to the SERS spectra of mannoproteins[28], which are considered to be the main components of the yeast cell wall. There are some other peaks attributed to amide, protein backbone and amino acid vibrations, related to the bioactivity of living cells such as protein secretion, movement, and so on[28]. These results demonstrate the potential of SHINERS as a safe and convenient technique for in-situ detection of cell wall proteins and as a possible probe of the dynamics and mechanisms of living systems.

SHINERS can also be used for inspecting food safety, drug security and environment protection accurately and rapidly. The shell-isolated nanoparticles could simply be spread as 'smart dust' over
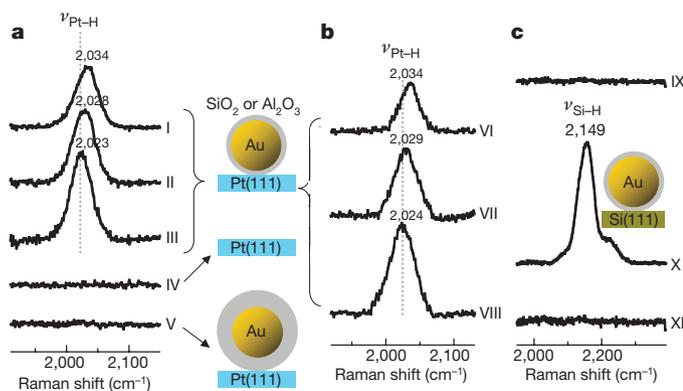

Figure 2 | Detection of hydrogen adsorption on single-crystal flat surfaces of Pt and Si by SHINERS. a, Potential-dependent SHINERS spectra of hydrogen adsorbed on a Pt(111) surface. Curve I, at −1.2 V; curve II, −1.6 V; curve III, −1.9 V; curve IV, without Au/SiO$_2$ nanoparticles; curve V, with the thicker shell nanoparticles at −1.9 V. **b**, Potential-dependent SHINERS spectra of hydrogen adsorbed on a Pt(111) surface using Au/Al$_2$O$_3$ nanoparticles. Curve VI, −1.2 V; curve VII, −1.6 V; curve VIII, −1.9 V. **c**, SHINERS spectra on Si(111) wafer treated with 98% sulphuric acid (curve IX), 30% HF solution (curve X) and O$_2$ plasma (curve XI).
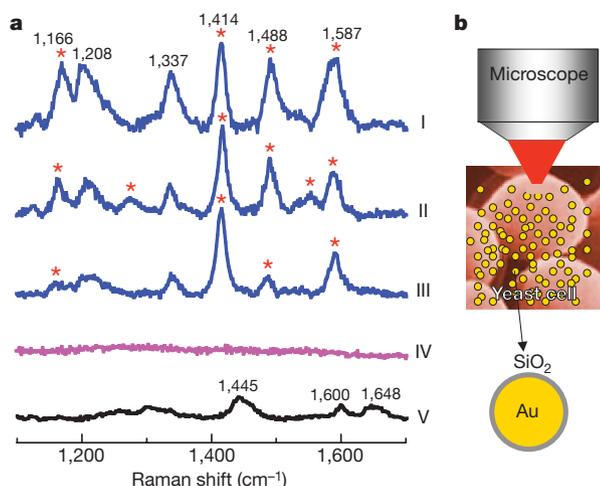
Figure 3 | *In situ* probing of biological structures by SHINERS. a, Curves I, II and III, SHINERS spectra obtained from different spots at the wall of an yeast cell incubated with Au/SiO$_2$ nanoparticles. Curve IV, the spectrum recorded from a substrate coated with Au/SiO$_2$ but without a yeast cell; curve V, a normal Raman spectrum for yeast cells. The peaks marked with red asterisks are closely related to mannoprotein. **b**, Schematic of a SHINERS experiment on living yeast cells. Laser power on the sample was 4 mW. The collected times were 60 s for curves I, II, III and IV and 600 s for curve V.

the probed surface and the measurement taken *in situ*. This approach could be used for inspecting pesticide residues on food and fruit. Figure 4 shows that normal Raman spectra recorded on fresh orange with clean pericarps (curve I) or contaminated by parathion (curve II) show only two bands at about 1,155 cm^{-1} and 1,525 cm^{-1}, attributed to carotenoid molecules contained in citrus fruits[29]. By spreading shell-isolated nanoparticles on the same surface, we can clearly detect two bands at 1,108 cm^{-1} and 1,341 cm^{-1} (curve III) that are characteristic bands of parathion residues[30]. The same result can also be obtained by using a portable Raman spectrometer (Supplementary Fig. 14). This demonstrates that SHINERS could have tremendous scope as a simple-to-use, field-portable and cost-effective analyser.

By changing the working mode from direct contact (SERS) or non-contact (TERS) to the shell-isolated mode, SHINERS avoids the
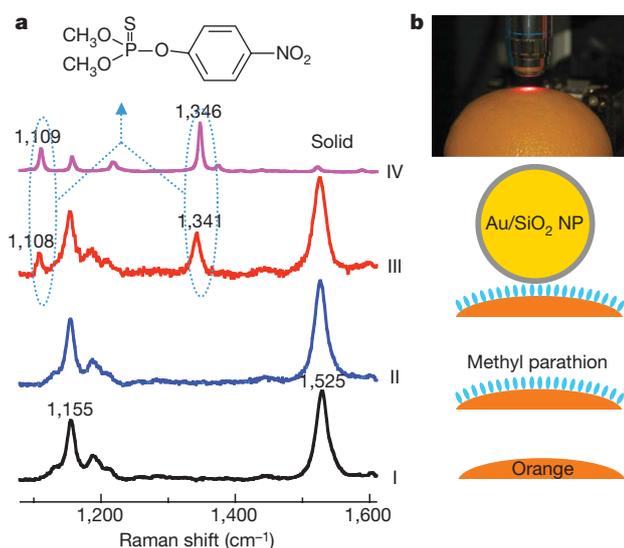

Figure 4 | *In situ* inspection of pesticide residues on food/fruit. a, Normal Raman spectra on fresh citrus fruits. Curve I, with clean pericarps; curve II, contaminated by parathion. Curve III, SHINERS spectrum of contaminated orange modified by Au/SiO$_2$ nanoparticles. Curve IV, Raman spectrum of solid methyl parathion. Laser power on the sample was 0.5 mW, and the collected times were 30 s. **b**, Schematic of the SHINERS experiment.

long-standing limitations (inaccessibility or difficulty) of SERS for the precise characterization of various materials, surfaces and biological samples. The use of a thin-shell coating around the SERS-active metal nanostructure has several benefits: it keeps the smart dust from agglomerating, protects the SERS-active nanostructure from contact with what is being probed, and allows the 'smart dust' to conform to different contours of samples. Given the availability of portable Raman spectrometers, our very simple method can be widely applied to probe surface composition, adsorption and processes of diverse objects and morphologies, from single-crystal surfaces to cell walls, from semiconductors to fruits. The concept of shell-isolated-nanoparticle enhancement may also be applicable to more general spectroscopy such as infrared spectroscopy, sum frequency generation and fluorescence. We anticipate that SHINERS will be developed into a simple, fast, non-destructive, flexible and portable characterization tool widely used in basic and applied research in the natural sciences, industry and even daily life.

METHODS SUMMARY

We first chemically synthesized Au nanoparticles with diameters of about 55 nm as cores using a standard sodium citrate reduction method[20], onto which ultrathin silica shells were coated to form Au core/silica shell (Au/SiO$_2$) nanoparticles[21]. To accelerate the synthesis procedure and make the uniformly ultrathin silica shell, we elevated the reaction temperature from room temperature to 90 °C (see Supplementary Methods for detailed information) The Au/Al$_2$O$_3$ core–shell nanoparticles were prepared mainly using the atomic layer deposition technique[5].

The structure and surface morphology of the core–shell nanoparticles and the shell thicknesses were measured by high-resolution transmission electron microscopy (HRTEM) (JEM 4000EX and Tecnai F30). Raman spectra were recorded on a LabRam I confocal microprobe Raman system (Jobin-Yvon). The excitation line was 632.8 nm from a He-Ne laser.

1. Nie, S. M. & Emory, S. R. Probing single molecules and single nanoparticles by surface enhanced Raman scattering. *Science* 275, 1102–1106 (1997).
2. Kneipp, K. *et al.* Single molecule detection using surface-enhanced Raman scattering (SERS). *Phys. Rev. Lett.* 78, 1667–1670 (1997).
3. Moskovits, M. Surface-enhanced spectroscopy. *Rev. Mod. Phys.* 57, 783–826 (1985).
4. Kneipp, K., Moskovits, M. & Kneipp, H. (eds) *Surface-enhanced Raman Scattering–Physics and Applications* (Springer, 2006).
5. Camden, J. P., Dieringer, J. A. & Van Duyne, R. P. Controlled plasmonic nanostructures for surface-enhanced spectroscopy and sensing. *Acc. Chem. Res.* 41, 1653–1661 (2008).
6. Baumberg, J. J. *et al.* Angle-resolved surface-enhanced Raman scattering on metallic nanostructured plasmonic crystals. *Nano Lett.* 5, 2262–2267 (2005).
7. Cao, Y. W. C., Jin, R. C. & Mirkin, C. A. Nanoparticles with Raman spectroscopic fingerprints for DNA and RNA detection. *Science* 279, 1536–1540 (2002).
8. Chen, Z. *et al.* Protein microarrays with carbon nanotubes as multicolor Raman labels. *Nature Biotechnol.* 26, 1285–1292 (2008).
9. Jain, P. K., Huang, X., El-Sayed, I. H. & El-Sayed, M. A. Noble metals on the nanoscale: optical and photothermal properties and some applications in imaging, sensing, biology, and medicine. *Acc. Chem. Res.* 41, 1578–1586 (2008).
10. Jackson, J. B. & Halas, N. J. Surface-enhanced Raman scattering on tunable plasmonic nanoparticle substrates. *Proc. Natl Acad. Sci. USA* 101, 17930–17935 (2004).
11. Graham, D., Thompson, D. G., Smith, W. E. & Faulds, K. Control of enhanced Raman scattering using a DNA-based assembly process of dye-coded nanoparticles. *Nature Nanotechnol.* 3, 548–551 (2008).
12. Qian, X. *et al. In vivo* tumor targeting and spectroscopic detection with surface-enhanced Raman nanoparticle tags. *Nature Nanotechnol.* 26, 83–90 (2008).
13. Anker, J. N. *et al.* Biosensing with plasmonic nanosensors. *Nature Mater.* 7, 442–453 (2008).
14. Tian, Z. Q., Ren, B., Li, J. F. & Yang, Z. L. Expanding generality of surface-enhanced Raman spectroscopy with borrowing SERS activity strategy. *Chem. Commun.* 34, 3514–3534 (2007).
15. Nie, S. M. & Zare, R. N. Optical detection of single molecules. *Annu. Rev. Biophys. Biomed.* 26, 567–596 (1997).
16. Park, S., Yang, P., Corredor, P. & Weaver, M. J. Transition metal-coated nanoparticle films: vibrational characterization with surface-enhanced Raman scattering. *J. Am. Chem. Soc.* 124, 2428–2429 (2002).
17. Tian, Z. Q. & Ren, B. Adsorption and reaction at electrochemical interfaces as probed by surface-enhanced Raman spectroscopy. *Annu. Rev. Phys. Chem.* 55, 197–229 (2004).
18. Stöckle, R. M., Suh, Y. D., Deckert, V. & Zenobi, R. Nanoscale chemical analysis by tip-enhanced Raman spectroscopy. *Chem. Phys. Lett.* 318, 131–136 (2000).

19. Pettinger, B., Ren, B., Picardi, G., Schuster, R. & Ertl, G. Nanoscale probing of adsorbed species by tip-enhanced Raman spectroscopy. *Phys. Rev. Lett.* **92**, 096101–096104 (2004).

20. Wu, D. Y., Li, J. F., Ren, B. & Tian, Z. Q. Electrochemical surface-enhanced Raman spectroscopy of nanostructures. *Chem. Soc. Rev.* **37**, 1025–1041 (2008).

21. Frens, G. Controlled nucleation for regulation of particle-size in monodisperse gold suspension. *Nature* **241**, 20–22 (1973).

22. Liz-Marzán, L. M., Michael, G. & Mulvaney, P. Synthesis of nanosized gold-silica core-shell particles. *Langmuir* **12**, 4329–4335 (1996).

23. Lu, Y., Yin, Y., Li, Z. Y. & Xia, Y. Synthesis and self-assembly of Au@SiO$_2$ core-shell colloids, *Nano Lett.* **2**, 785–788 (2002).

24. Mulvaney, S. P., Musick, M. D., Keating, C. D. & Natan, M. J. Glass-coated, analyte-tagged nanoparticles: a new tagging system based on detection with surface-enhanced Raman scattering. *Langmuir* **19**, 4784–4790 (2003).

25. Smith, W. E. Practical understanding and use of surface enhanced Raman scattering/surface enhanced resonance Raman scattering in chemical and biological analysis. *Chem. Soc. Rev.* **37**, 955–964 (2008).

26. Sherry, L. J. *et al.* Localized surface plasmon resonance spectroscopy of single silver nanocubes. *Nano Lett.* **5**, 2034–2038 (2005).

27. Ren, B. *et al.* In situ monitoring of Raman scattering and photoluminescence from silicon surfaces in HF aqueous solutions. *Appl. Phys. Lett.* **72**, 933–935 (1998).

28. Sujith, A. *et al.* Surface enhanced Raman scattering analyses of individual silver nanoaggregates on living single yeast cell wall. *Appl. Phys. Lett.* **92**, 103901 (2008).

29. Schulte, F., Mader, J. & Kroh, L. W. Panne, U. & Kneipp, J. Characterization of pollen carotenoids with in situ and high-performance thin-layer chromatography supported resonant Raman spectroscopy. *Anal. Chem.* **81**, 8426–8433 (2009).

30. Lee, D. *et al.* Quantitative analysis of methyl parathion pesticides in a polydimethylsiloxane microfluidic channel using confocal surface-enhanced Raman spectroscopy. *Appl. Spectrosc.* **60**, 373–377 (2006).

Author Contributions Z.Q.T., Z.L.W., J.F.L. and B.R. conceived and designed the experiments, analysed the results and participated in writing the manuscript. J.F.L., Y.F.H., Y.D., S.B.L., X.S.Z., F.R.F., W.Z. and Z.Y.Z. performed the experiments and analysed the results. Z.L.Y. and D.Y.W contributed to theoretical calculations.

Author Information Reprints and permissions information is available at www.nature.com/reprints. The authors declare no competing financial interests. Correspondence and requests for materials should be addressed to Z.Q.T. (zqtian@xmu.edu.cn) and Z.L.W. (zhong.wang@mse.gatech.edu).